

Thermodynamic Stability of Interfacial Gaseous States

Xue Hua Zhang,^{*,†} Nobuo Maeda,^{*,‡} and Jun Hu^{§,||}

Department of Chemical and Biomolecular Engineering, The University of Melbourne, Victoria 3010, Australia, CSIRO molecular and health technologies, Clayton, Victoria 3168, Australia, Nanobiology Laboratory, Bio-X Life Science Research Center, College of Life Science and Biotechnology, Shanghai Jiaotong University, Shanghai 200030, China, and Shanghai Institute of Applied Physics, Chinese Academy of Sciences, P.O. Box 800-204, Shanghai 201800, China

Received: August 22, 2008; Revised Manuscript Received: September 10, 2008

We studied the thermodynamic stability of interfacial gaseous states on atomically smooth highly ordered pyrolytic graphite (HOPG) in water using atomic force microscopy. Quasi-two-dimensional gas layers (micropancakes) required a higher supersaturation of gas than spherical-cap-shaped nanobubbles. The two forms of gas coexisted at a sufficiently high supersaturation of gas where one or more of the nanobubbles may sit on top of a micropancake. The micropancakes spontaneously coalesced with each other over time. After the coalescence of two neighboring micropancakes which each had had a nanobubble on top, one nanobubble grew at the expense of the other. We analyzed these results assuming temporal and local quasi-equilibrium conditions.

The free energy per unit area in which water is in contact with a smooth hydrophobic surface always increases upon formation of a gas layer, regardless of the contact angle of water on the solid surface.¹ Despite this undisputable thermodynamic fact, there has been intense research effort focusing on the study of interfacial nanobubbles, as reviewed by Attard.² This may be because, in part, there is considerable scientific merit in identifying a condition for possible existence of such interfacial gas layers or establishing a reliable protocol to induce such entities. Stabilization of foams in coatings and removal of parasites in fish ponds using gaseous pesticides, to name a few, could greatly benefit from such study.

Our systematic study on interfacial gaseous states has recently identified such conditions which in essence showed that different types of interfacial gaseous states could exist in an aqueous phase if it was sufficiently supersaturated with a gas.^{1,3–8} These research efforts firmly established the protocols for inducing spherical-cap-shaped nanobubbles on a solid substrate and also led to recent detection of novel and more surprising quasi-two-dimensional “micropancakes” on HOPG.⁹

The established methods for the formation of spherical-cap nanobubbles and flat gas micropancakes induce supersaturation of gas next to a solid surface in one way or another.⁹ The methods include displacement of an organic solvent such as ethanol with water, displacement of warm water ($\approx 40^\circ\text{C}$) with cold water ($\approx 0^\circ\text{C}$), or generation of a temperature gradient by pre- or in situ heating of the substrate.⁹ These induced gaseous entities can be removed from the surface by injection of predegassed water to the system or by direct exposure of the

system to reduced pressure (≈ 0.1 atm).⁹ Equipped with the reliable experimental protocols, here, we studied the stability of this novel gaseous state on HOPG using atomic force microscopy. In contrast to spherical-cap nanobubbles which have been reported to exist at many different surfaces,^{1,3,7,8,10–13} gas micropancakes have so far been detected only on HOPG.⁹ We do not know the reason for this yet, but it is likely to be related to the atomically smooth surface of HOPG *within a cleavage step* where a micropancake forms (other substrates are substantially rougher to such an extent that the roughness becomes comparable to the height of micropancakes). Regardless, the nanobubbles and micropancakes on atomically smooth HOPG surfaces provide an excellent model system for which meaningful thermodynamic analyses can be made.

Water was purified using a Mill-Q unit (Millipore Corporation, Boston, MA). Ethanol (>99.9%), methanol (>99.9%), 1-propanol (>99.9%), 2-propanol (>99%), and 1-butanol (>99%) were all obtained from Chinese Chemical Reagent Company (Shanghai, China). Freshly cleaved HOPG (ZYH, NT-MDT, Moscow, Russia) was used as a substrate. The Multimode Nanoscope IIIa and IV AFM equipped with a liquid cell (Digital Instruments Veeco Metrology Group, NY) was used for the imaging in the tapping mode. The probe was silicon nitride with a nominal spring constant of 0.32 N/m (NP-S, Digital Instruments Veeco Metrology Group, NY). The AFM tips were cleaned by acetone, ethanol, and water in this order before use. The fluid cell and the O-ring were cleaned with ethanol and water and dried with a prefiltered air stream. In our previous work,⁹ we described in detail how to get stable tapping mode AFM images of nanobubbles and micropancakes on HOPG surfaces. In brief, the set point ratio was set above 0.9. The scan rate was usually faster than $5\ \mu\text{m/s}$ because it was difficult to obtain quality images, especially of pancakes, at slower scan rates. The experimental temperature was about 23°C .

* Corresponding authors. E-mail: xuehuaz@unimelb.edu.au (X.H.Z.); Nobuo.Maeda@csiro.au (N.M.).

[†] The University of Melbourne.

[‡] CSIRO molecular and health technologies.

[§] Shanghai Jiaotong University.

^{||} Chinese Academy of Sciences.

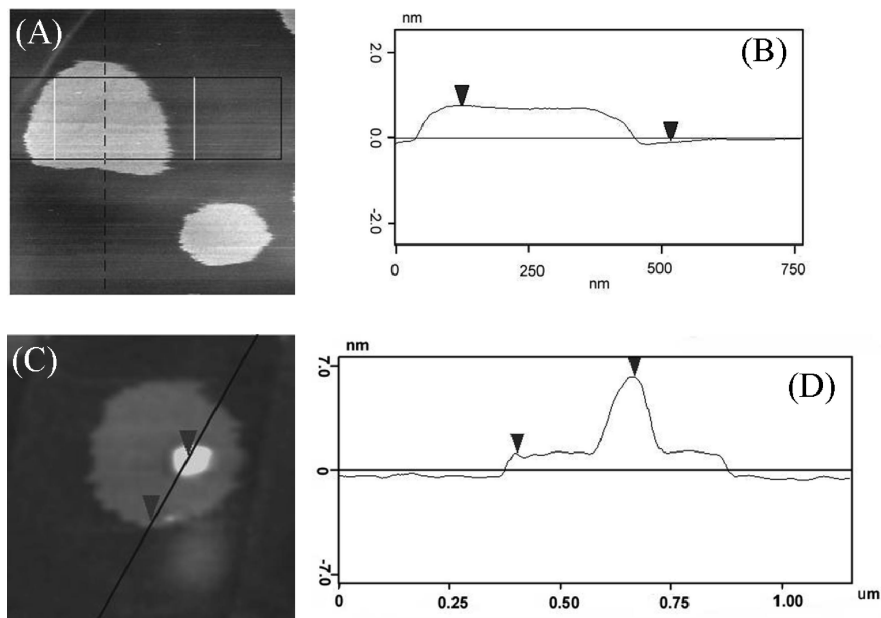


Figure 1. AFM images of micropancakes and bubble–micropancake composites on freshly cleaved HOPG. (A) A height image of micropancakes. The scan size is $800\text{ nm} \times 800\text{ nm}$. (B) Height profile of the larger micropancake in part A along the width of the black rectangle drawn in part A. The profile was averaged over the height of the rectangle. The locations of the two arrows correspond to the height averages over the two vertical white lines shown in part A. The average height of the micropancake is less than 2 nm. The height of a micropancake did not exceed 5 nm. (C) A height image of a micropancake with a nanobubble on the top. The scan size is $1\text{ }\mu\text{m} \times 1\text{ }\mu\text{m}$. (D) Cross-sectional profile of the micropancake–nanobubble composite in part C. The cross section was taken along the black line shown in part C. The locations of the two arrows correspond to those of the two arrows in part C.

Interfacial gaseous phases were formed by the solvent exchange method.⁹ Briefly, the substrate under study was exposed to (1) water, (2) an organic solvent such as ethanol, and then (3) water again. The plausible mechanism behind this protocol is discussed in refs 1, 4, 9, and 14. We note at this stage that the system is well sealed and it is assumed that the moderate level of supersaturation of gas achieved by this protocol is maintained in the system throughout the time scale of a given experimental run (up to several hours). This solvent exchange method has an advantage over other methods such as displacement of warm water with cold water or generation of a temperature gradient by pre- or in situ heating of the substrate. The solvent exchange method is easier in practice and also provides us with a greater degree of control through extra adjustable experimental parameters such as choice of different organic solvents which have a range of solubility of gas, the flow rate and the temperature of liquids, the concentrations of such solvents in water, and pH and the ionic strength of the aqueous phase. We will detail the effect of such parameters elsewhere.

From our several hundreds of AFM images of micropancakes, we found that the height of micropancakes never exceeded 5 nm (typically 1–2 nm; see Figure 1). Due to this proximity of the substrate and the resulting surface forces exerting on the oscillating tip, the exact height of a micropancake may be influenced by imaging conditions, such as the spring constant of a cantilever and the imaging force, so here we quote the upper bound. The lateral dimension of micropancakes, on the other hand, varied from several hundred nanometers to tens of microns. Thus, the aspect ratio was about 3 orders of magnitude. An example of composites of micropancakes and nanobubbles, i.e., nanobubbles sitting on top of micropancakes, is shown in Figure 1C and D. When a sample surface was imaged on randomly selected locations, the number of nanobubbles sitting on a micropancake was usually one or none. Only occasionally we detected more than one nanobubble sitting on a pancake.

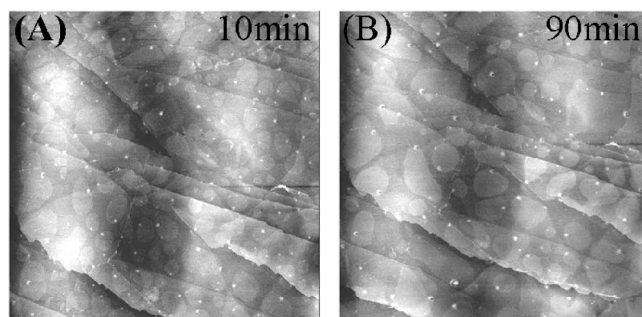


Figure 2. Time evolution of nanobubbles and micropancakes on HOPG: (A) Initial micropancakes (10 min after the formation); (B) 90 min later of the same region as part A. The scan size is $5\text{ }\mu\text{m} \times 5\text{ }\mu\text{m}$. The micropancakes moved closer to each other, and some had coalesced with each other over time. As a result, the average size of a micropancake increased with time.

The height of these nanobubbles varied from 1 nm to several tens of nanometers. The lateral size was from tens to hundreds of nanometers. The cross-sectional analyses of these nanobubbles revealed the profile of a part of an arc, suggesting the spherical-cap shape of the bubbles. The contact angle formed by the nanobubbles on the micropancake can be calculated to be about 155° , so measured through the aqueous phase. This is close to the contact angle of nanobubbles directly sitting on a bare HOPG surface.¹ We note at this stage that the Laplace pressure inside such a nanobubble was found to be in the range 1.1–1.4 atm.¹⁴

After the formation, micropancakes laterally spread and coalesced over time, as shown in Figure 2. Interestingly, we found that the nanobubbles on top of micropancakes had a tendency to localize near the edge of the underlying micropancakes. This is a peculiar phenomenon, and the physical reason behind this tendency is not clear at this stage. It has been known that HOPG has hydrophobic and hydrophilic moieties in the vicinity of cleavage steps,¹⁵ and micropancakes would spread

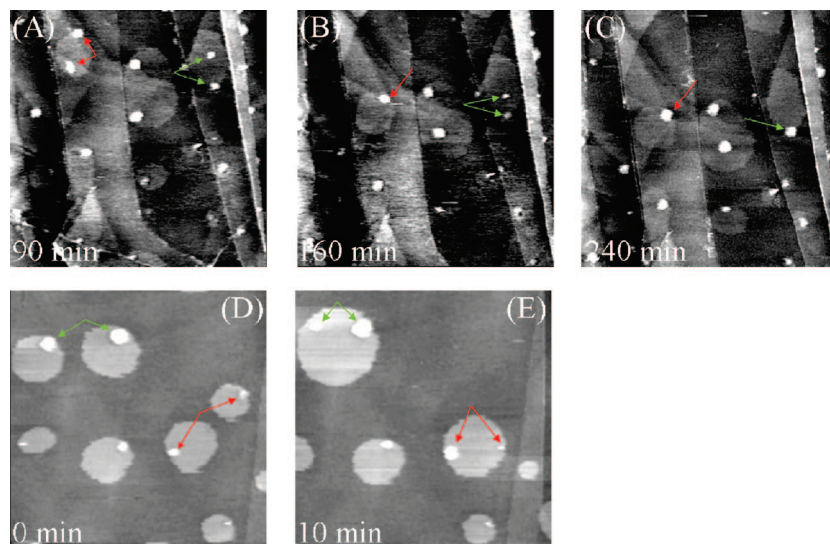


Figure 3. Time evolution of nanobubbles on the top of pancakes in water (A–C) and in 1 M Na₂SO₃ solution (D, E). The scan size of all the images is $2.5\ \mu\text{m} \times 2.5\ \mu\text{m}$. The arrows indicate the nanobubbles on top of coalesced micropancakes which underwent Ostwald ripening. Arrows of different colors refer to different pairs of nanobubbles that underwent separate Ostwald ripening processes. Note that some other nanobubbles on top of isolated micropancakes or a pair of nanobubbles that had very similar sizes on a micropancake remain virtually unchanged during the same period.

along with hydrophobic moieties and avoid hydrophilic ones. Then, it would be tempting to speculate that the localization of nanobubbles near the edge of micropancakes is a result of preferential spreading of micropancakes to particular directions on HOPG which had nucleated from nanobubbles. However, there were instances that a nanobubble had been near the center of a micropancake and then migrated to an edge later.

After the coalescence of two neighboring micropancakes which each had had one nanobubble on top, the coalesced larger micropancake now had two nanobubbles on top, as shown in Figure 3. Very interestingly, when the size of these two nanobubbles was different, the larger nanobubble soon started growing at the expense of the smaller one. It appeared that the rate of the Ostwald ripening was much faster between two nanobubbles on top of the same micropancake compared with those on separate micropancakes. This may be a reflection of a faster diffusion rate of gas molecules in a *continuous* gas phase than through an aqueous phase. In light of this result, it is likely that the occasional detection of multiple nanobubbles on a single micropancake in an image of a randomly selected surface location was a reflection of a “snapshot” of a transient state in which one of the nanobubbles was growing at the expense of the others. We note that while the nanobubbles on top of the micropancakes that had coalesced grew or shrank, the other nanobubbles on top of isolated micropancakes had changed little during the same period (Figure 3). Thus, there is hardly any net transfer of gas between a nanobubble and the underlying micropancake until it coalesced with another micropancake.

The flatter shape of micropancakes compared with that of nanobubbles means a larger gas–aqueous interfacial area for a micropancake than for a nanobubble for a given amount of gas. It follows that, for a given amount of gas, the interfacial free energy cost (surface tension) to the formation of a micropancake would be greater than that of a nanobubble. Then, a reduction in the interfacial free energy cost would be greater for a micropancake than for a nanobubble when a solvent of a lower surface tension is used during the final stage of the solvent exchange procedure (in the place of pure water). However, this is contrary to what we observed; i.e., when ethanol was displaced with a dilute (2 vol %) ethanol solution during the

final stage of the solvent exchange procedure, micropancakes no longer formed, whereas nanobubbles still formed. Given that the solubility of gas in an ethanol solution is greater than that in water, the inference is that the interfacial free energy must be of secondary importance compared to the bulk (supersaturation) free energy.²²

When nanobubbles and micropancakes in water, so formed by the usual solvent exchange protocol, were subsequently subject to dilute ethanol aqueous solutions which act as “gas sinks”, micropancakes still persisted in 0.15 vol % ethanol solution. Further increase in the ethanol concentration eventually destroyed all micropancakes above 5 vol % and all nanobubbles above 20 vol %. This result shows that not only formation of micropancakes requires a higher supersaturation of gas than that of nanobubbles, but also removal of nanobubbles requires a greater reduction of supersaturation of gas than that of micropancakes. This result thus shows that (1) the disappearance of the gaseous entities must be primarily due to a reduction in the supersaturation of gas in ethanol solutions compared to that in water and (2) the reduction in the gas supersaturation leads to a smaller reduction in the overall free energy for micropancakes than for nanobubbles (i.e., the free energy of micropancakes becomes higher than that of nanobubbles at a low supersaturation of gas).

The mere presence of nanobubble–micropancake composites suggests that the overall chemical potential of gas inside a nanobubble must be similar to that inside a micropancake at a sufficiently high supersaturation of gas. Then, we may be able to describe the interfacial gaseous states in quasi-equilibrium terms.¹⁶ This is to assume a system that is not in the global free energy minimum can be in a temporal and/or local equilibrium state. This approach enables us to predict the direction of a change of a system based on a hypothetical change in the free energy associated with an infinitesimal variation of a parameter of interest (principle of virtual work). Once we assume quasi-static conditions, it becomes meaningful to analyze the pressure of nanobubbles in terms of the Laplace pressure and that of micropancakes in terms of the disjoining pressure.^{17,18} Then, the free energies of nanobubbles and micropancakes are functions of supersaturation in the surrounding aqueous phase

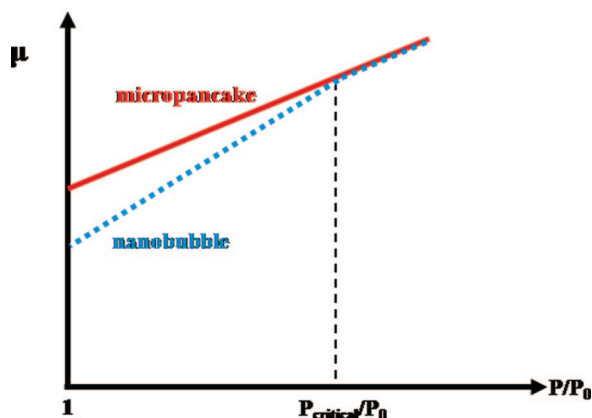


Figure 4. Schematic free energy profiles of nanobubbles and micropancakes.

as well as of their respective characteristic sizes; $\mu_{\text{nanobubble}} = \mu_{\text{nanobubble}}(P/P_0, \text{radius})$ and $\mu_{\text{micropancake}} = \mu_{\text{micropancake}}(P/P_0, \text{thickness})$, where μ is the chemical potential of a gas molecule, P is the pressure of the gas, and P_0 is the saturation pressure of the gas. Then, our results suggest the presence of a supersaturation threshold of a gas below which $\mu_{\text{nanobubble}}$ becomes lower than $\mu_{\text{micropancake}}$ and above which they are the same. We schematically depict this picture in Figure 4.

Our results on the Ostwald ripening of nanobubbles on top of a coalesced micropancake suggest that, at this particular level of supersaturation of gas, the chemical potential inside the shrinking nanobubble becomes greater than that inside the underlying micropancake which in turn is greater than that inside the growing nanobubble ($\mu_{\text{shrinking nanobubble}} > \mu_{\text{micropancake}} > \mu_{\text{growing nanobubble}}$). On the other hand, Figure 3 shows that while the nanobubbles on top of the micropancakes that had coalesced grew or shrank, the other nanobubbles on top of isolated micropancakes had hardly changed during the same period. Moreover, when two nanobubbles sitting on a micropancake happened to have a very similar size to each other, these two nanobubbles coexisted for a very long time (a few hours) on the micropancake. Thus, generally, $\mu_{\text{nanobubble}} = \mu_{\text{micropancake}}$, that is, until the underlying micropancakes coalesced with each other. The question is how can $\mu_{\text{nanobubble}}$, which used to be equal to $\mu_{\text{micropancake}}$, suddenly assume a higher ($\mu_{\text{shrinking nanobubble}}$) or a lower ($\mu_{\text{growing nanobubble}}$) chemical potential upon coalescence of underlying micropancakes. It cannot be attributed to the difference in the pressure of gas between a nanobubble and a micropancake, because they were the same prior to the coalescence and there is no physical reason which suggests that the pressure of a smaller nanobubble can suddenly jump *and at the same time* that of a larger nanobubble can suddenly drop upon coalescence of underlying micropancakes.

This is a challenging situation. Our proposed solution is that the free energy of gas inside nanobubbles or micropancakes may need to be decoupled into two components, one that depends on the bulk term and the other that depends on the interfacial term. Then, the Ostwald ripening of the nanobubbles may be driven solely by this interfacial component of the free energy while the pressure inside the three parties remains unchanged all the time. This interfacial component of the free energy could be reduced by reducing the interfacial area through a change in shape. This could be achieved by putting the gas that had been in two separate nanobubbles together into one larger nanobubble while keeping the radii of curvature and the pressure the same (this is possible if different contact angles are allowed). Importantly, for nanobubbles of different sizes

(on different micropancakes) to be able to coexist with the micropancakes and the surrounding aqueous media, *both before and after the coalescence of a pair of micropancakes*, the bulk (pressure) term of nanobubbles must be the same. Our proposed decoupling of interfacial and bulk components of the free energy is novel, but it is compatible with the existing framework of thermodynamics. In fact, it would be difficult to account for all aspects of our results without this kind of assumption.

Finally, we show that the thickness and the pressure of gas inside a micropancake remain unchanged during the Ostwald ripening process and that all micropancakes must have the same thickness and gas pressure under a given P/P_0 . We often observed laterally spreading micropancakes. In the absence of the disjoining pressure, when a unit amount of gas is added to a micropancake, the energetically least costly way to accommodate the excess gas would be to slightly increase its thickness because, given the very flat shape of the micropancake, the increase in the surface area could be kept minimal that way. The experimentally observed lateral spreading of a pancake thus suggests that the contribution from the disjoining pressure to the overall free energy (which suppresses the growth in the thickness) is dominant compared with the surface tension which would oppose an increase in the interfacial area. We do not know *a priori* a mathematical form of the disjoining pressure of a micropancake as a function of its thickness. Nevertheless, our results on the Ostwald ripening of two nanobubbles on a micropancake show that the gas that is feeding the growing nanobubble must be coming from the shrinking one. Then, it follows that the thickness of the micropancake cannot be increasing during the Ostwald ripening process (if it were, then where did the gas that is feeding the growing nanobubble come from?). Likewise, the thickness of a micropancake cannot be decreasing either (if it were, then why did the smaller nanobubble shrink at all?). Thus, our analyses show that the disjoining pressure of a micropancake must be a steep function of thickness with a well-defined minimum. We can conclude this *despite our inability to measure the thickness of a micropancake with sufficient precision*.

One may ask if such a well-defined minimum in the disjoining pressure is physically plausible. We note that it is not only plausible but also such a system of comparable scale does exist. The lower density and dielectric constant of a gas than those of water mean the attractive van der Waals forces for the gas micropancake systems (solid substrate–gas film–liquid). Such attractive van der Waals forces are known to hinder growth in thickness.¹⁹ In fact, one of us previously pointed out that this, when combined with the large oscillatory structural component of the disjoining pressure of a thin film, is precisely the mechanism underlying the otherwise mysterious observation in surface freezing of linear alkanes,²⁰ where the thickness of a solid hydrocarbon film remains *precisely monomolecular* with decreasing temperature toward the bulk freezing point.²¹

Acknowledgment. X.H.Z. acknowledges the support by the Australian Research Council (Australian Postdoctoral Fellowship, DP0880152). Travel was funded by the Particulate Fluids Processing Centre, an ARC Special Research Centre. J.H. acknowledges the support by the Science and Technology Ministry of China (No. 2007CB936003).

References and Notes

- (1) Zhang, X. H.; Maeda, N.; Craig, V. S. J. *Langmuir* **2006**, *22*, 5025–5035.
- (2) Attard, P. *Adv. Colloid Interface Sci.* **2003**, *104*, 75–91.
- (3) Lou, S. T.; Ouyang, Z. Q.; Zhang, Y.; Li, X. J.; Hu, J.; Li, M. Q.; Yang, F. J. *J. Vac. Sci. Technol., B* **2000**, *18*, 2573–2575.

- (4) Zhang, X. H.; Zhang, X. D.; Lou, S. T.; Zhang, Z. X.; Sun, J. L.; Hu, J. *Langmuir* **2004**, *20*, 3813–3815.
- (5) Zhang, X. H.; Li, G.; Maeda, N.; Hu, J. *Langmuir* **2006**, *22*, 9238–9243.
- (6) Yang, S. J.; Dammer, S. M.; Bremond, N.; Zandvliet, H. J. W.; Kooij, E. S.; Lohse, D. *Langmuir* **2007**, *23*, 7072–7077.
- (7) Yang, J. W.; Duan, J. M.; Fornasiero, D.; Ralston, J. J. *Phys. Chem. B* **2003**, *107*, 6139–6147.
- (8) Zhang, L. J.; Zhang, Y.; Zhang, X. H.; Li, Z. X.; Shen, G. X.; Ye, M.; Fan, C. H.; Fang, H. P.; Hu, H. *Langmuir* **2006**, *22*, 8109–8113.
- (9) Zhang, X. H.; Zhang, X.; Sun, J.; Zhang, Z.; Li, G.; Fang, H.; Xiao, X.; Zeng, X.; Hu, J. *Langmuir* **2007**, *23*, 1778–1783.
- (10) Ishida, N.; Inoue, T.; Miyahara, M.; Higashitani, K. *Langmuir* **2000**, *16*, 6377–6380.
- (11) Holmberg, M.; Kuhle, A.; Garnaes, J.; Mørch, K.; Boisen, A. *Langmuir* **2003**, *19*, 10510–10513.
- (12) Steitz, R.; Gutberlet, T.; Hauss, T.; Klosgen, B.; Krastev, R.; Schemmel, S.; Simonsen, A. C.; Findenegg, G. H. *Langmuir* **2003**, *19*, 2409–2418.
- (13) Paxton, W. F.; Kistler, K. C.; Olmeda, C. C.; Sen, A.; St Angelo, S. K.; Cao, Y. Y.; Mallouk, T. E.; Lammert, P. E.; Crespi, V. H. *J. Am. Chem. Soc.* **2004**, *126*, 13424–13431.
- (14) Zhang, X. H.; Khan, A.; Ducker, W. A. *Phys. Rev. Lett.* **2007**, *98*, 136101.
- (15) Yang, S.; Kooij, E. S.; Poelsema, B.; Lohse, D.; Zandvliet, H. J. W. *Europhys. Lett.* **2008**, 81.
- (16) Li, Z. X.; Zhang, X. H.; Zhang, L. J.; Zeng, X. C.; Hu, J.; Fang, H. *J. Phys. Chem. B* **2007**, *111*, 9325–9329.
- (17) Adamson, A. W.; Gast, A. P. *Physical Chemistry of Surfaces*; John Wiley & Sons, Inc.: New York, 1997.
- (18) Derjaguin, B. V.; Churaev, N. V.; Muller, V. M. *Surface Forces*; Consultants Bureau: New York, 1987.
- (19) Mahanty, J.; Ninham, B. W. *Dispersion Forces*; Academic Press: London, 1976.
- (20) Maeda, N.; Yaminsky, V. V. *Int. J. Mod. Phys. B* **2001**, *15*, 3055–3077.
- (21) Ocko, B. M.; Wu, X. Z.; Sirota, E. B.; Sinha, S. K.; Gang, O.; Deutsch, M. *Phys. Rev. E* **1997**, *55*, 3164.
- (22) The change in the interfacial free energy upon removal of a gas layer on a solid in a liquid per unit area is $\Delta G = \gamma_{sl} - \gamma_{sg} - \gamma_{lg}$, where γ is the interfacial free energy and the subscripts s, l, and g refer to solid, liquid, and gas phases. Using the Young equation, $\Delta G = -\gamma_{lg} - \gamma_{lg} \cos \theta = -\gamma_{lg}(1 + \cos \theta)$. The contact angle of water on freshly cleaved HOPG is $\approx 80^\circ$ ($\cos \theta \approx 0.17$), that of ethanol is small ($\cos \theta \approx 1$), the surface free energy of water is about $\gamma_{lg} = 72 \text{ mJ/m}^2$, and that of ethanol is about $\gamma_{lg} = 22 \text{ mJ/m}^2$ for the experimental temperature. Substituting these numbers yields $\Delta G_{\text{water}} \approx -72(1 + 0.17) = -84 \text{ mJ/m}^2$ and $\Delta G_{\text{ethanol}} \approx -22(1 + 1) = -44 \text{ mJ/m}^2$. All ethanol solutions have intermediate ΔG values. Now we know that micropancakes existed in water *despite this greater incentive for micropancakes to disappear*. The inevitable conclusion is that the interfacial free energy is of secondary importance.

JP807515F